Optimization of Beclin 1-targeting stapled peptides by staple scanning leads to enhanced anti-proliferative potency in cancer cells

Qifan Yang[1,2][†], Xianxiu Qiu[3,4,5][†], Xiaozhe Zhang[3,4], Yingting Yu[3,4], Na Li[3,4], Xing Wei[4,6], Guoqin Feng,[1,2] Yan Li,[1,2] Yanxiang Zhao[3,4*] and Renxiao Wang[1,2*]

[1]*Department of Medicinal Chemistry, School of Pharmacy, Fudan University, Shanghai, 200433 P. R. China*

[2]*State Key Laboratory of Bioorganic and Natural Products Chemistry, Center for Excellence in Molecular Synthesis, Shanghai Institute of Organic Chemistry, Chinese Academy of Sciences, Shanghai 200032, P. R. China*

[3]*The Hong Kong Polytechnic University Shenzhen Research Institute, Shenzhen 518057, P.R. China*

[4]*Department of Applied Biology and Chemical Technology, State Key Laboratory of Chemical Biology and Drug Discovery, The Hong Kong Polytechnic University, Hung Hom, Kowloon, Hong Kong, P. R. China*

[5]*Guangdong Provincial Key Laboratory of Medical Molecular Diagnostics, Dongguan Key Laboratory of Medical Bioactive Molecular Developmental and Translational Research, Guangdong Medical University, Dongguan523808, P.R. China*

[6]*Department of Obstetrics and Gynecology, The Second Affiliated Hospital of Xi'an Jiaotong University, Xi'an 710004, P.R. China*

[†]These authors contributed equally to this work.

[*]Correspondence should be addressed to Y.Z. (yanxiang.zhao@polyu.edu.hk) and R.W. (wangrx@fudan.edu.cn).

Abstract (250 words)

Beclin 1 is a scaffolding member of the Class III Phosphoinositol-3-kinase (PI3KC3) complex and is essential for PI3KC3-mediated cellular processes including autophagy and endolysosomal trafficking. Beclin 1 is also a haplo-insufficient tumor suppressor and frequently deleted in human sporadic breast, ovarian and prostate cancer. Beclin 1 recruits two PI3KC3 regulators Atg14L and UVRAG through its coiled coil domain to form Atg14L/UVRAG-containing PI3KC3 complex with up-regulated kinase activity. Our previous work has shown that the Beclin 1 coiled coil domain forms a metastable homodimer that readily dissociates upon binding of Atg14L or UVRAG to form a stabilized Beclin 1-Atg14L/UVRAG heterodimer. We developed hydrocarbon-stapled peptides that bound to Beclin 1 coiled coil domain with moderate affinity, reduced Beclin 1 homodimerization and promoted Beclin 1-Atg14L/UVRAG interaction. These peptides also induced autophagy and enhanced endolysosomal degradation of cell surface receptors like EGFR. Here we present optimization of these Beclin 1-targeting peptides by staple scanning and sequence permutation. Our results show that placing the hydrocarbon staple closer to the Beclin 1-peptide interface enhanced the binding affinity by ~10-30 fold. Compared to other autophagy inducers like rapamycin and Tat-Beclin 1 peptide, our optimized peptides show the unique profile of not only inducing autophagy but also significantly enhancing the endolysosomal degradation of cell surface receptors EGFR and HER2, leading to potent anti-proliferative efficacy in cancer cells that over-expresses these oncogenic "drivers". Given the importance of EGFR and HER2 signaling pathways in cancer cell proliferation, our Beclin 1-targeting stapled peptides may serve as effective therapeutic candidates for EGFR- or HER2-driven cancer.

Introduction

Beclin 1 (Bcl-2 interacting coiled coil protein 1) is an evolutionarily conserved mammalian protein with homologs identified in eukaryotes ranging from yeast and plants to *C. elegans*, fruit flies and zebrafish (1). Initially discovered as a Bcl-2 interacting protein in a yeast two-hybrid screen, Beclin 1 has later been confirmed to be an indispensable member of the mammalian Class III phosphatidylinositol 3-kinase (PI3KC3) complex (2-4). PI3KC3 is a multi-protein assembly with a core unit formed by three molecules including Beclin 1, the lipid kinase Vps34 (Vacuolar Protein Sorting 34) that specifically phosphorylates phosphatidylinositols (PIs) at the 3' hydroxyl position of the inositol ring to generate PI3Ps; and a serine/threonine kinase Vps15 (Vacuolar Protein Sorting 15) that constitutively associates with Vps34 as a stable binding partner. PI3KC3 serves as the major producer of phosphatidylinositol-3-phosphates (PI3Ps) in mammalian cells and is essential for cellular processes that involve PI3P-enriched membrane vesicles including autophagy, endolysosomal trafficking and phagocytosis (3, 4). As a critical regulator of the PI3KC3 complex, Beclin 1 has been functionally implicated in a variety of physiological processes such as glucose metabolism, embryonic development and innate immunity. Deficiency or dysfunction of Beclin 1 has been linked to human pathologies such as cancer and neurodegenerative diseases (1, 5-7).

Extensive studies have confirmed Beclin 1 as a haplo-insufficient tumor suppressor intimately involved in tumorigenesis. Beclin 1 is monoallelically deleted in 40–75% of cases of human sporadic breast, ovarian, and prostate cancer (8). Heterozygous knockout of Beclin 1 in mice leads to higher rate of spontaneous malignancies such as lymphomas and lung or hepatocellular carcinomas (8, 9). Additionally, cell surface oncogenic receptors

such as Epidermal Growth Factor Receptor (EGFR) in non-small-cell lung cancer (NSCLC) and Human Epidermal Growth Factor Receptor 2 (HER2) in breast cancer can associate with Beclin 1 to suppress autophagy and promote tumorigenesis (10, 11). Furthermore, induction of autophagy by over-expressing a Beclin 1 F121A mutant that doesn't bind to its inhibitor Bcl-2 has been shown to enhance autophagy and abrogate tumorigenesis in transgenic mice that over-express HER2 (11). Notably, Tat-Beclin 1, a peptide that contained the HIV Tat sequence for cell penetration and a segment of 11 amino acids from the evolutionarily conserved region of Beclin 1 (residue 269 to 279) showed potent anti-proliferative effect in mice xenograft model of HER2-positive (HER2+) human breast tumor, with efficacy comparable to the clinically used HER2 inhibitor lapatinib (11). These genetic and pharmacological findings suggest that targeting Beclin 1 may serve as an effective anti-proliferative strategy for EGFR- or HER2-driven cancer.

Structural studies from our lab and others have delineated the molecular mechanism of how Beclin 1 promotes the activity of the PI3KC3 complex. As the scaffolding molecule, Beclin 1 directly recruits two positive regulators Atg14L and UVRAG in mutually exclusive manner to form Atg14L- or UVRAG-containing PI3KC3 complexes with significantly enhanced lipid kinase activity to promote PI3KC3-dependent processes (12-14). The Beclin 1-Atg14L/UVRAG interaction relies critically on their respective coiled coil domains. In particular, our studies reveal that the Beclin 1 coiled coil domain forms a metastable homodimer because its hydrophobic dimer interface is significantly weakened by several "imperfect" polar or charged residues (15). The metastable Beclin 1 homodimer readily dissociates upon Atg14L/UVRAG binding and transits into highly stable heterodimeric Beclin 1-Atg14L/UVRAG complex with a coiled coil interface significantly strengthened by hydrophobic pairings and electrostatically complementary interactions

(16). Harnessing the metastable feature of Beclin 1 coiled coil domain, we have developed a series of hydrocarbon-stapled peptides that specifically bind to this region to reduce Beclin 1 homodimerization and enhance the Beclin 1-Atg14L/UVRAG interaction. These designed peptides also showed efficacy in terms of inducing autophagy and promoting the endolysosomal degradation of cell surface receptors like EGFR (16).

Given the functional importance of Beclin 1 in tumorigenesis, we reason our rationally designed Beclin 1-targeting stapled peptides may inhibit the proliferation of EGFR- or HER2-driven cancer cells by enhancing autophagy and promoting the endolysosomal degradation of EGFR and HER2. However, the peptides developed in our previous study had moderate *in vitro* binding affinity to Beclin 1 with $K_d \sim$ 6-60 μM and showed little cytotoxicity in multiple NSCLC cell lines. Here we report optimization of our previously designed peptides by implementing new staples and residue mutations to enhance their binding affinity to Beclin 1. Our results reveal that placing the hydrocarbon staple close to the Beclin 1 coiled coil surface strengthened the Beclin 1-peptide interaction by roughly 10~30 folds. These newly designed peptides showed significantly enhanced anti-proliferative potency in HER2+ cancer cells through promotion of autophagy and endolysosomal degradation of EGFR and HER2. Our results suggest that Beclin 1-targeting stapled peptides that can serve as potential therapeutic agents for HER2-driven cancer.

RESULTS

Molecular design and modeling of stapled peptides targeting Beclin 1

The template peptide sequence for designing the stapled peptides reported in our previous study was an 11-residue segment including residues 191–205 on the Beclin 1 coiled coil domain. This segment, termed Native-P1 by us, was chosen because our previous structural studies revealed that it formed part of the Beclin 1 homodimer interface but did not overlap with the binding site for UVRAG (16). Thus, Native-P1 is expected to bind to the Beclin 1 coiled coil domain to reduce its homodimerization and promote the Beclin 1-Atg14L/UVRAG heterodimeric complex, subsequently leading to enhanced autophagy and endolysosomal trafficking.

The Native-P1 peptide is assumed to form an α-helical structure when binding to the Beclin 1 coiled coil domain (Figure 1a). In this study, a hydrocarbon staple was used to link two residues on the Native-P1 sequence that were separated by six residues so that the staple could cross two rounds of helical circle to stabilize the peptide structure. We attempted six possible scaffolds for installing this hydrocarbon staple (Figure 1b), all of which kept the four residues critical for binding (i.e. L192, L196, V199, and R203) undisturbed. We also modified the chemical structure of the hydrocarbon staple by replacing the α-methyl group of the unnatural amino acids used in our previous study with α-hydrogen (Figure 1c). The smaller-sized α-hydrogen group helped to afford more conformational flexibility and reduce possible steric clash when the hydrocarbon staple wa positioned at different locations along the peptide (i7-01s to i7-06s as shown in Figure 1b). During our MD simulations, the helical structures of all six stapled peptides were maintained especially between residues L192 to R203 (Supplementary Figure S1). Although our MD simulations, 100 ns long for each, were not extensive enough to reach real conformational convergence, the predicted binding energies of all six stapled peptides

indicated that i7-01s, i7-02s, i7-04s, and i7-06s tended to form more stable interactions with the Beclin 1 coiled coil domain (Supplementary Figure S2).

Among them, we chose the i7-01s scaffold for further analysis because in this case, E195 and N202 on Native-P1 were mutated to install the hydrocarbon staple, both of which were near the hydrophobic region on the surface of the coiled coil domain (Figure 2). Thus, this mutation may reduce the unfavorable hydrophobic-hydrophilic mismatch between the peptide and the coiled coil domain. Besides, according to our predicted model, the staple on i7-01s actually stacks on the surface of the coiled coil domain, which may further enhance the binding of this stapled peptide. Based on the i7-01s scaffold, we then conducted systematic single-point mutations on the Native-P1 sequence. The predicted binding energies of all of those mutated peptides indicated that mutations at Q194, E197, D198, E200, K201, K204, and K205 were more likely to improve binding affinity (Supplementary Figure S3). We then manually selected and combined certain favorable single-point mutants into new designs of multiple-point mutants, in a hope to achieve even higher binding affinity. Binding energies for all 75 peptides designed are summarized in Supplementary Table S1. The average binding energy of most of them (72 in 75) is more favorable than that of the Native-P1 peptide based on the same i7-01s scaffold, which meet our expectation on molecular design.

Newly designed peptides with the i7-01s scaffold show significantly higher binding affinity to Beclin 1 *in vitro*

Based on a balanced consideration of the predicted binding mode and binding affinity as well as the physicochemical properties of the peptide (such as the total charge),

we finally selected a total of 17 stapled peptides among all designs for chemical synthesis (Figure 3a). Binding affinity of all 17 newly synthesized peptides to the Beclin 1 coiled coil domain was measured in an Isothermal Titration Calorimetry (ITC) assay (Table 1, Figure 3a and Supplementary Figure S4). Compared to SP4, which was the best-affinity stapled peptide ($K_d = 3.2$ μM) obtained in our previous study, 12 of these newly synthesized peptides exhibit comparable or stronger binding to Beclin 1. In particular, two peptides (i.e. i7-01s-20 and i7-01s-31) have binding affinity stronger than SP4 by roughly 10 and 30 folds, respectively. Our molecular modeling results suggest that the hydrocarbon staple on the newly obtained peptides is closer to the coiled coil domain surface instead of stretching into the solvent as in the case of SP4 (Figure 2), which is a major factor accounting for their enhanced binding affinity. In summary, our new design strategy combining staple scanning and mutation scanning has yielded a collection of stapled peptides with promising activities at least in the *in vitro* binding assay.

….(Figure 3b)

Optimized Beclin 1-targeting stapled peptides effectively induce autophagy

We decided to focus on i7-01s-20 and i7-01s-31, the two new peptides with strongest binding affinity to Beclin 1, for subsequent functional characterization. We first used trypan blue exclusion assay to confirm that both i7-01s-20 and i7-01s-31 showed negligible cytotoxicity on HEK293T cells at 10- and 20-μM concentrations respectively, after 24 h of treatment (Supplementary Figure S5).

The impact of these two peptides on cellular autophagic activity was examined by detecting the protein levels of LC3 and p62, two molecular markers of autophagy. During

the autophagy process, cytosolic protein LC3 is converted from its *apo* form (LC3-I) to the lipidated form (LC3-II) for accumulation on autophagosomes. Thus an increase in LC3-II level is regarded as a reliable indicator of elevated cellular autophagic activity. Similarly, p62 is an autophagy receptor that is degraded in the lysosome together with autophagic substrates. A decrease in p62 level is also commonly used as an indicator for higher autophagic activity, although some studies have shown that p62 is not as sensitive as LC3-II. Our results show that treatment of HEK293T cells with i7-01s-31 at 10 and 20 μM for 3 hours induced noticeable albeit small increase in LC3-II levels by (Figure 4a & 4b). Such increase became significantly stronger in the presence of the chloroquine (CQ), a lysosomal inhibitor (Figure 4a & 4c). The protein level of p62 did not show any noticeable change after peptide treatments, either in the presence or absence of CQ (Figure 4a, 4d & 4e). Given that p62 may be less sensitive than LC3-II in terms of detecting autophagic flux, it is possible the small change in p62 couldn't be reliably detected by western blot. This pattern of change in LC3-II and p62 levels is comparable to what was observed for Tat-SP4 as reported in our previous study (15). Thus, the newly designed peptides i7-01s-20 and i7-01s-31, although showing ~10-30 fold stronger binding affinity to Beclin 1 than Tat-SP4, actually induce autophagy with comparable efficacy.

Optimized Beclin 1-targeting stapled peptides significantly enhance endolysosomal degradation of EGFR and HER2

As a scaffolding member of the PI3KC3 complex, Beclin 1 is essential for multiple PI3KC3-dependent processes including autophagy, endolysosomal trafficking and phagocytosis. To assess the efficacy of our newly designed peptides on the endolysosomal trafficking process, the ligand-induced endolysosomal degradation of cell surface receptors HER2 and EGFR was characterized by western blotting using SKBR3 breast cancer cell

line that over-expresses both EGFR and HER2. In SKBR3 cells, treatment by the agonist EGF triggered slow degradation of EGFR and HER2, with ~50% remaining even after 24 hours (Figure 5a, 5d & 5e). Tat-SP4 treatment at 2 μM didn't show any noticeable impact on the degradation profile (Figure 5b, 5d & 5e). In contrast, i7-01s-31 treatment at 2μM resulted in significant reduction of HER2 level, with ~50% decrease at 15 hours post EGF stimulation, and ~70% decrease at 24 hours (Figure 5c & 5d). i7-01s-31 treatment also strongly promoted EGFR degradation, with approximately 60% reduction at 15 hours post EGF stimulation (Figure 5c & 5e).

To further compare the potency of the newly designed peptides to Tat-SP4, we repeated the EGFR and HER2 degradation assays using higher concentrations of Tat-SP4. We found that the concentration of Tat-SP4 should be elevated to 20- or 40-μM to achieve similar degradative effect on HER2 and EGFR levels (Supplementary Figure S6). Our data indicate that the newly designed peptides with enhancing binding affinity to Beclin 1 also show significantly higher efficacy in terms of promoting endolysosomal trafficking of HER2 and EGFR.

Optimized Beclin 1-targeting stapled peptides potently inhibit proliferation of HER2+ cancer cells

To evaluate the anti-proliferative potency of our newly designed peptides on EGFR- or HER2-driven cancer, we used trypan blue exclusion assay to measure the IC_{50} values of our peptides on SKBR3 cells. Our results show that while Tat-SP4 exerts a moderate anti-proliferative effect with IC_{50} of 33.68 μM, both i7-01s-20 and i7-01s-31 are ~2-5 times more potent with IC_{50} values of 13.55 μM and 7.12 μM for i7-01s-31,

respectively (Figure 6a). Similarly, a five-day proliferation assay confirms that while Tat-SP4 reduced proliferation of SKBR3 cells by ~30% at 20 μM (Figure 6b), i7-01s-20 treatment at 20μM, or i7-01s-31 treatment at 10μM, showed much higher dosage-dependent potency to completely abolish cell proliferation (Figure 6c & 6d). These findings confirm that that newly designed stapled peptides inhibited proliferation of SKBR3 with significantly higher potency as compared to Tat-SP4.

Optimized Beclin 1-targeting stapled peptides induce necrotic cell death

Given the potent anti-proliferative efficacy of the newly designed peptides, we set out to investigate the molecular mechanism of this process. Observation during the trypan blue exclusion assays confirm that SKBE3 cells underwent cell death, not cell growth arrest, after treatment by i7-01s-31. To investigate whether the peptide-induced cell death was associated with apoptosis, flow cytometry with annexin V and propidium iodide (PI) staining was performed in SKBR3 cells. Annexin V labelled with the FITC fluorophore specifically labels phosphatidylserine (PS), a marker for apoptosis because this membrane lipid is normally located on the inner leaflet of the plasma membrane but flips to the outer leaflet during apoptosis. Thus an increase in Annexin V staining is a reliable and specific indicator of apoptosis. PI is a nucleic acid binding dye that labels cells after necrotic cell death because it can only reach the nucleus upon loss of plasma membrane integrity, a hallmark feature of necrosis. In contrast, Our flow cytometry data indicate that treatment by doxorubicin, a chemotherapeutic agent known to induce apoptosis, led to significant increase of Annexin V positive cells, confirming that apoptosis is the major cause of cell death (Figure 7a). In contrast, treatment by Beclin 1-targeting peptides, either Tat-SP4 or the newly developed i7-01s-31, only led to significant increase of PI positive staining cells but no increase of Annexin V positive cells. Furthermore, the extent of necrotic cell death

is dosage-dependent and correlates well with the potency of the peptide used, with i7-01s-31 inducing ~30% PI positive cells at 10 μM while Tat-SP4 only induced ~8% at same concentration (Figure 7a). In summary, our Beclin 1-targeting peptides induce necrotic cell death without indication of apoptosis. Whether such necrotic cell death is caused by elevated autophagic activity or rapid degradation of EGFR and HER2 receptors need to be further investigated.

…… (Figure 7b)

Discussion and Conclusions

Designing peptides with a hydrocarbon staple to reinforce their α-helical structure has served as an effective strategy to generate molecular prototypes capable of specific binding to target proteins (17). The first and most notable example of this strategy is the development of hydrocarbon-stapled peptides that targeted Bcl-2 family proteins to promote apoptosis in cancer cells. Walensky et. al. in 2004 showed that adding a hydrocarbon staple to a peptide representing the short BH3 helix of the pro-apoptotic BID protein enabled it to retain the α-helical structure, bind to anti-apoptotic Bcl-2 and Bcl-xL proteins *in vitro* at the same site as BID, and suppress proliferation of leukemia cells *in vivo* through induction of apoptosis (18). Follow-up studies from the same group and others demonstrated that stapled peptides mimicking BH3 helixes from other Bcl-2 family proteins such as BAD, BIM, MCL-1 and PUMA all showed similar function in terms of specific binding to their respective target, induction of apoptosis, and anti-proliferative efficacy in multiple cancer models (19-23). This strategy has also been successfully applied to a variety of protein targets involved in diverse human diseases such as cancer related MDM2/MDMX, β-catenin and NOTCH (24-28); the gap protein and integrase of HIV

virus (29-32); plus glucokinase, estrogen receptor and glucagon-like peptide-1 receptor (GLP-1) involved in cellular metabolism (33-35).

The potency of a stapled peptide in modulating a specific biological activity is influenced by many factors. The most important consideration is to ensure that the α-helical peptide, with its hydrocarbon staple, fits tightly and specifically to the intended binding site on the target protein. To achieve strong and specific binding, the amino acid sequence of the peptide is always subject to systematic scanning to identify residues that best fit onto the binding site of the target protein. For the hydrocarbon staple, the common approach is to place this moiety away from the intended binding site to avoid possible interference (17). Interestingly, several studies have reported that a hydrocarbon staple placed at the edge of the binding interface can actually help strengthen the protein-peptide interaction by complementary hydrophobic interactions with the target protein (23, 27, 28).

Here we present data to show that this strategy of placing the hydrocarbon staple close to the protein-peptide binding interface can help enhance the binding affinity and biological activity of Beclin 1-targeting stapled peptides. The Beclin 1 coiled coil domain, forms a long α-helix with extended surface that lacks a well-defined binding site (15). The prototype peptides reported in our previous study were constructed as a short three-round amphipathic helix with 11 residues, thus affording only three hydrophobic residues (L192, L196 and V199) to interact directly with Beclin 1 coiled coil interface (Figure 2a). In this study, we conducted "staple scanning" to explore all possible positions to install the hydrocarbon staple on the α-helical peptide. Our molecular modeling results show that placing the staple close to the edge of the Beclin 1-peptide binding interface as in the i7-01s scaffold allows it to rest on the hydrophobic region on the molecular surface of Beclin

1 (Figure 2b). Additionally, placing hydrophobic residues on the two helical turns within the span of the hydrocarbon staple is also beneficial for Beclin 1 binding. For the two lead peptides i7-01s-20 and i7-01s-31 that showed strongest binding affinity to Beclin 1, four out of the six residues between R8 and S5 are hydrophobic. In comparison, placing polar or charged residues at corresponding positions led to varied outcome with some showing comparable binding affinity to Tat-SP4 (i7-01s-02, -10, -12 etc.) while others showing significantly weakened binding such as i7-01s-54 and i7-01s-64 with $K_d \sim 300$ uM or no binding at all (i7-01s-30, -34 and -36) (Table 1). Overall, our study suggests that for stapled peptides targeting coiled coil domains that lack conventional binding sites, placing the hydrocarbon staple closer to the coiled coil surface and adding hydrophobic residues near the staple may be an effective approach to enhance their binding affinity by effectively expanding the hydrophobic binding interface.

Although Beclin 1 is well regarded as a tumor suppressor, pharmacological targeting of Beclin 1 or the Beclin 1-mediated autophagy process for cancer therapy has been challenging. Extensive studies have delineated the functional role of autophagy in cancer as a double-edged sword, exerting both anti- and pro-tumor effect in context-dependent manner (36-40). Thus, simply enhancing or blocking autophagy may not yield sufficient clinical efficacy. Indeed, several clinical trials testing the anti-cancer efficacy of hydroxychloroquine, a commonly used autophagy inhibitor, showed inconclusive results (41-43). Here we present an alternative approach to modulate Beclin 1 activity in cancer cells using stapled peptides that bind to the Beclin 1 coiled coil domain with optimized specificity and potency. In particular, with their binding affinity to Beclin 1 strengthened by ~10-30 fold, these new peptides significantly enhanced the endolysosomal degradation of cell surface oncogenic receptors EGFR and HER2, likely attenuating their downstream

signaling as well. Given that EGFR or HER2-driven cancer cells particularly rely on EGFR and HER2 signaling pathways to sustain proliferation and metastasis, they may be exceptionally sensitive to our Beclin 1-targeting peptides. The exact molecular processes that underpin such sensitivity are likely to be complex and difficult to quantify. Interestingly, our designed peptides induced necrotic cell death in HER2+ cancer cells instead of apoptosis. Whether this necrotic cell death is caused by the significantly enhanced degradation of HER2 and EGFR will need to be investigated in future studies.

In summary, through staple scanning and sequence optimization, we have developed Beclin 1-targeting stapled peptides that showed ~10-30 fold higher binding affinity to Beclin 1 *in vitro* and ~2-5 fold stronger anti-proliferative potency in HER2 positive cancer cells *in vivo* as compared to the prototype reported in our previous study. Our approach of targeting the Beclin 1 coiled coil domain with hydrocarbon-stapled peptides to enhance both autophagy and endolysosomal trafficking may be an effective therapeutic strategy for EGFR- or HER2-driven cancer.

Experimental section

Reagents and antibodies. Chloroquine (CQ; Sigma-Aldrich), Epidermal Growth Factor (EGF; Gibco), Protease inhibitor cocktail (Roche Diagnostics), Trypsin (Invitrogen), isopropyl-β-D-thiogalactopyranoside (IPTG; Sigma-Aldrich), anti-β-actin antibody (Santa Cruz Biotechnology), anti-LC3 antibody (Abnova), anti-p62 antibody (Abnova), anti-EGFR antibody (Santa Cruz Biotechnology), anti-HER2 antibody (Cell Signaling Technology), Anti-Mouse IgG-HRP (Sigma-Aldrich)，Anti-Rabbit IgG-HRP (Sigma-Aldrich).

Computational design of stapled peptides targeting Beclin 1

The α-helical segment (residues 191-205) on the coiled coil domain of Beclin 1 (PDB entry 3Q8T) was truncated as the template for designing stapled peptides binding to the Beclin 1 coiled coil domain. Molecular models of all stapled peptides were constructed by using the MOE software (version 2019, released by the Chemical Computing Group). In this study, a linear hydrocarbon staple was added to connect two anchor residues that were separated by six residues (i.e. the *i*th and the *i*th+7 residues) on the template peptide sequence. A total of six pairs of anchor residues were considered (Figure 1), including **i7-01s** (connecting E195 and N202), **i7-02s** (connecting R191 and D198), **i7-03s** (connecting D198 and V205), **i7-04s** (connecting Q194 and K201), **i7-05s** (connecting E197 and K204), and **i7-06s** (connecting I193 and E200).

In this study, we chose the i7-01s scaffold to perform mutations on the Native P1 sequence *in silico* in order to obtain new peptides with higher binding affinity. Except for the two anchor residues (i.e. E195 and N202), there are 13 residues on the Native-P1 sequence for possible mutation. Each of those 13 residues was mutated into the other 19 natural amino acid residues, which resulted in a total of $13 \times 20 = 260$ peptides. The complex model of each stapled peptide was derived directly from the model of i7-01s in complex with the Beclin 1 coiled coil domain. Those designed stapled peptide were subjected to molecular dynamics simulation and binding energy prediction (see the section below for technical details). Based on the predicted binding energies, we then manually selected and combined certain favorable single-point mutants into new designs of multiple-point mutants to further enhance the interactions with the Beclin 1 coiled coil domain. This effort led to a total of 75 stapled peptides with multiple mutations (fewer than five points)

on the Native-P1 sequence. Among them, we finally selected 17 for chemical synthesis based on a balanced consideration of their predicted binding mode and binding affinity as well as their physicochemical properties (such as the total charge). Note that every designed stapled peptide was capped at the N- and C-terminal by an acetyl group and an amino group, respectively, in our molecular modeling.

Molecular simulation of stapled peptides to Beclin 1

Molecular dynamics (MD) simulations were employed to evaluate the interactions between the Beclin 1 coiled coil domain and the designed stapled peptides. All computations were conducted by using the CPU-version of the AMBER18 software or the GPU-version of the AMBER16 software. Beclin 1 as well as the stapled peptides were treated with the AMBER FF14SB force field. In particular, the hydrocarbon staple on each designed peptide was technically treated as two unnatural amino acid residues (i. e. R8G and S5G) connected by a double bond: R8G consisted of seven methylene units stemming from the alpha-carbon on the peptide backbone in the R-configuration; whereas S5G consisted of four methylene units stemming from another alpha-carbon on the peptide backbone in the S-configuration. The atomic charges assigned on these two unnatural residues were computed at the HF/6-31G* level with the Gaussian 09 software and then derived by using the restrained electrostatic potential (RESP) method in the AMBER software.
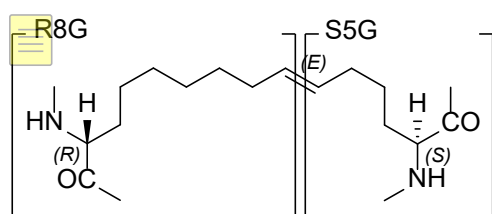
In this work, we used the crystal structure of the coiled coil domain of Beclin 1 (PDB entry 3Q8T) as the starting point for MD simulation. For the sake of convenience, the coiled coil domain was truncated to keep the segment between V213 and K264 only. The segment

between R191 to V205 on the same crystal structure was truncated as the template for building the designed stapled peptides. The model of each stapled peptide was built by mutating certain residues into the desired ones. The resulting initial complex model was energetically minimized to release clashes between the stapled peptide the coiled coil domain. Then, the complex model was soaked in a cubic box filling with TIP3P water molecules. The whole system was prepared and energetically minimized through a multi-step process as described in our previous study (16). After minimization, the whole system was heated from 0 *K* to 300 *K* in 100 *ps* and then equilibrated for 500 *ps* under a constant pressure of 1 *atm*. Then, the resulting system was subjected to a MD simulation of 100 *ns* long. Three parallel simulations were conducted for each peptide to enhance conformational sampling. Technical settings of the above MD simulation process was also the same as in our previous work (41).

Binding energy of each stapled peptide to the Beclin 1 coiled coil domain was evaluated by using the Molecular Mechanics Generalized-Born Surface Area (MM-GB/SA) module in the AMBER software. The basic settings for applying MM-GB/SA were also the same as in our previous study (41). In this work, the binding energy of each stapled peptide was computed based on the last 20 *ns* section on the corresponding MD trajectory. Note that the configurational entropy term in the MM-GB/SA equation was not computed in this work because we assumed this part was roughly the same for all peptides under consideration.

Chemical synthesis of stapled peptides. All peptide samples were purchased from *GL Biochem (Shanghai) Ltd.* Generally, the peptides were synthesized by automated solid-phase peptide synthesis, incorporating olefin-containing amino acids at the designated

positions. Then, the hydrocarbon staple was formed on olefin-containing amino acids by ring-closing metathesis reaction using the Grubbs catalyst. Similar to our previous study (41), a cell-penetrating Tat sequence (YGRKKRRQRRR) was added to the N-terminal of each peptide to assist with intracellular delivery. Chemical structure and purity of the final products were characterized by HRMS and HPLC. Purity of each synthesized peptides is > 95%. Stock solution of each obtained peptide was prepared by dissolving the sample in pure water to a concentration of 20 mM.

Protein expression and purification. The expression and purification of Beclin 1 coiled coil domain was performed as described previously (15). Briefly, the coiled coil domain of human Beclin 1 (residues 176-268) was cloned into the modified pET32a vector containing the human rhinovirus (HRV) 3C protease cleavage site and thioredoxin-6xHis fusion tag. Recombinant protein for the Beclin 1 coiled oil domain was expressed in *Escherichia coli* BL21(DE3) and purified by Ni^{2+}-NTA affinity chromatography (HisTrap HP, GE Healthcare) first and followed by size-exclusion chromatography (Superdex 75, GE Healthcare).

Isothermal Titration Calorimetry (ITC). ITC assays were carried out by MicroCal PEAQ-ITC Automated (Marvern) at 25 °C. All designed peptides and purified protein for the Beclin 1 coiled coil domain were dialyzed into the buffer containing 50 mM Tris, 150 mM NaCl at pH 7.4. For each titration assay, the injection syringe was loaded with 40 µl of peptide and the cell was loaded with Beclin 1 CC protein. Typically, titrations consisted of 19 injections, and each injection was performed at a time interval of 180 seconds to ensure that the titration peak returned to the baseline. The titration data were analyzed using the MicroCal PEAQ-ITC Analysis software and fitted by the one-site binding model.

Cell culture. HEK283T and SKBR3 cell lines were cultured in DMEM (Gibco, Grand Island, NY, USA) supplemented with 10% fetal bovine serum (Life Technologies), 1% penicillin G (100 U/ml), and streptomycin (100 mg/ml), and in a humidified incubator at 37 °C with 5% CO_2. All cell lines used in the experiments were mycoplasma detected negative by MycoAlert[TM] PLUS Mycoplasma Detection Kit (Lonza) before and during the experiment.

Cell viability assay. Cell viability was measured by trypan blue exclusion assay following the standard protocol provided by the manufacturer. SKBR3 cells were seeded on 96-well plates containing complete medium at a density of 1×10^4 cells per well. Upon cell attachment, cells were treated with the indicated stapled peptide, chemical reagents, or vehicle control for 24 hours. Afterwards, the number of trypan blue positive staining cells and the number of total cells were manually counted under a light microscope (Olympus). Cell viability is calculated as the number of viable cells divided by the total number of cells. All experiments were repeated in triplicate and the mean was calculated.

Co-immunoprecipitation

To examine Beclin 1 self-association and Beclin 1-Atg14L/UVRAG interaction in vivo, HEK293T cells were transfected with GFP-tagged Beclin 1 and/or the indicated Flag-tagged constructs. After transfection for 48 hours, cells were lysed with lysis buffer (25 mM HEPES PH 7.5, 10 mM MgCl2, 150 mM NaCl, 1 mM EDTA.2Na, 1% Nonidet P-40, 1% Triton X-100, 2% glycerol, and EDTA-free protease inhibitor cocktail). Cell lysate was centrifuged at 14,000 rpm at 4 °C for 10 min, and then the supernatant was aliquoted and incubated with the indicated concentration of peptide, anti-Flag antibody (Sigma-Aldrich) and Protein A/G Agarose beads (Santa Cruz Biotechnology, sc-2003) at 4 °C

overnight. Following incubation, the agarose beads were washed three times with the lysis buffer, denatured in SDS loading buffer at 100 °C for 10 min, and analyzed by immunoblot analysis.

Immunoblot analysis. Whole cell lysates were extracted using Laemmli sample buffer (62.5 mM Tris-HCl, pH 6.8, 2% SDS, 25% glycerol, 5% β-mercaptoethanol) supplemented with EDTA-free protease inhibitor cocktail (Roche). Protein concentration was determined using a standard Bradford assay before immunoblotting. Protein samples were separated by SDS–PAGE, transferred to a PVDF membrane (Millipore, USA), and incubated with the primary antibodies and HRP-conjugated secondary antibodies. Protein bands were visualized using ECL reagents. β-actin was used as the loading control.

EGFR/HER2 degradation assay. HEK293T or SKBR3 cells in 6-well plate were washed with PBS two times and serum-starved overnight in DMEM medium. Endocytosis of EGFR and HER2 were induced by treatment with 200ng/mL of EGF at 37 °C. Cells were collected at the indicated time after EGF stimulation and lysed as described in immunoblot analysis.

Flow cytometry. The degree of cellular apoptosis and necrosis was assessed by flow cytometry following the standard protocol provided by the manufacturer. Briefly, SKBR3 cells after the indicated peptide treatment were harvested by trypsin, labelled with Annexin V and PI (Invitrogen), subjected to flow cytometer system (BD Accuri C6), and analyzed by BD Accuri C6 software. The cell populations could be distinguished by the staining of Annexin V /PI. Typically, cellular population in the lower left quadrant is live cells (Annexin V^-, PI^-), the lower right quadrant represents early apoptotic cells (Annexin V^+,

PI$^-$), the upper right quadrant represents late apoptotic cells (Annexin V$^+$, PI$^+$), the upper left quadrant represents necrotic cells (Annexin V$^-$, PI$^+$).
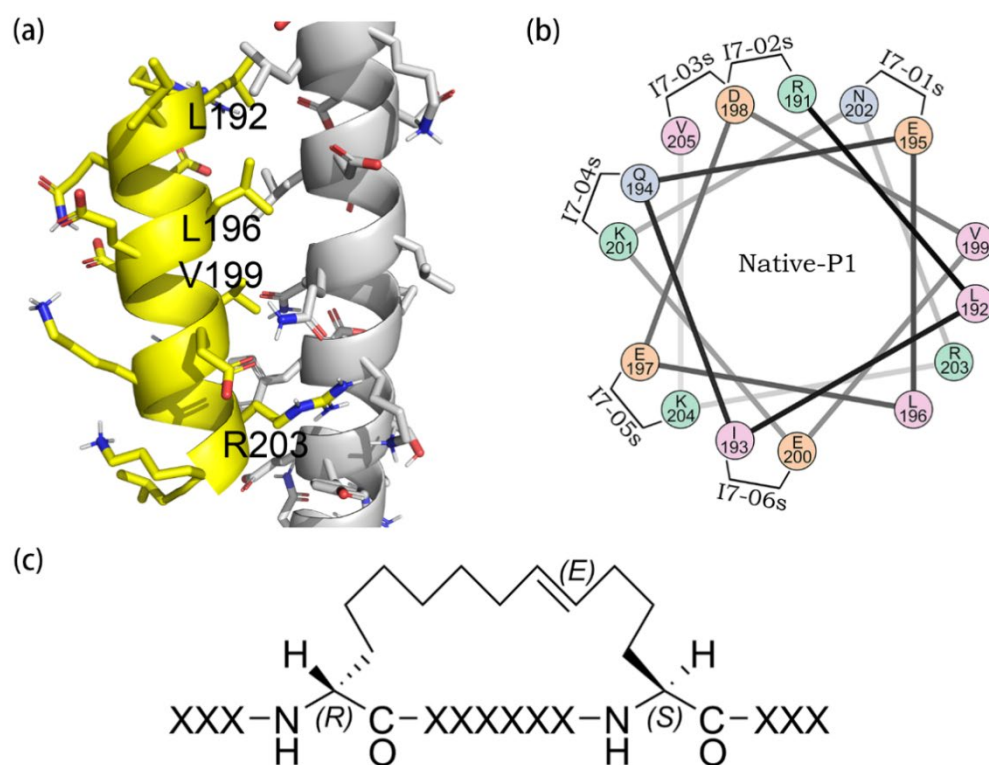
Figure 1. Illustration of how the hydrocarbon staple was installed on the peptide sequence. (a) Molecular model of the native-P1 peptide (in yellow) in complex with the Beclin 1 coiled-coil domain (in gray, from PDB entry 3Q8T). Here, Native-P1 is assumed to be in a helical structure for binding. This complex model was used as the template for deriving the initial model of all designed stapled peptides described in this study. (b) Staple position scanning in peptide design. The hydrocarbon staple was added at six positions on the Native-P1 sequence. (c) Chemical structure of the hydrocarbon staple. Two amino acids containing olefin side chains were separated by six residues on the peptide sequence. The two side chains were connected by a Ruthenium-catalyzed ring-closing metathesis reaction, resulting in the 11-carbon long linker shown in this figure.
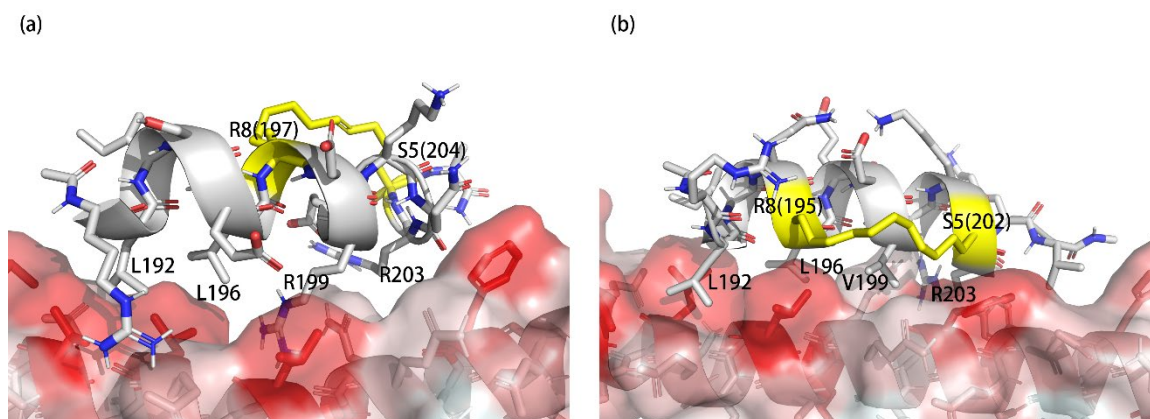
Figure 2. Predicted binding mode to Beclin 1 coiled-coil domain of (a) the stapled peptide SP4 obtained in our previous study and (b) the newly designed i7-01s scaffold. Here, the hydrocarbon staple is colored in yellow. The molecular surface of the Beclin 1 coiled-coil domain is colored by the hydrophobicity scale, where the region in darker red is more hydrophobic.
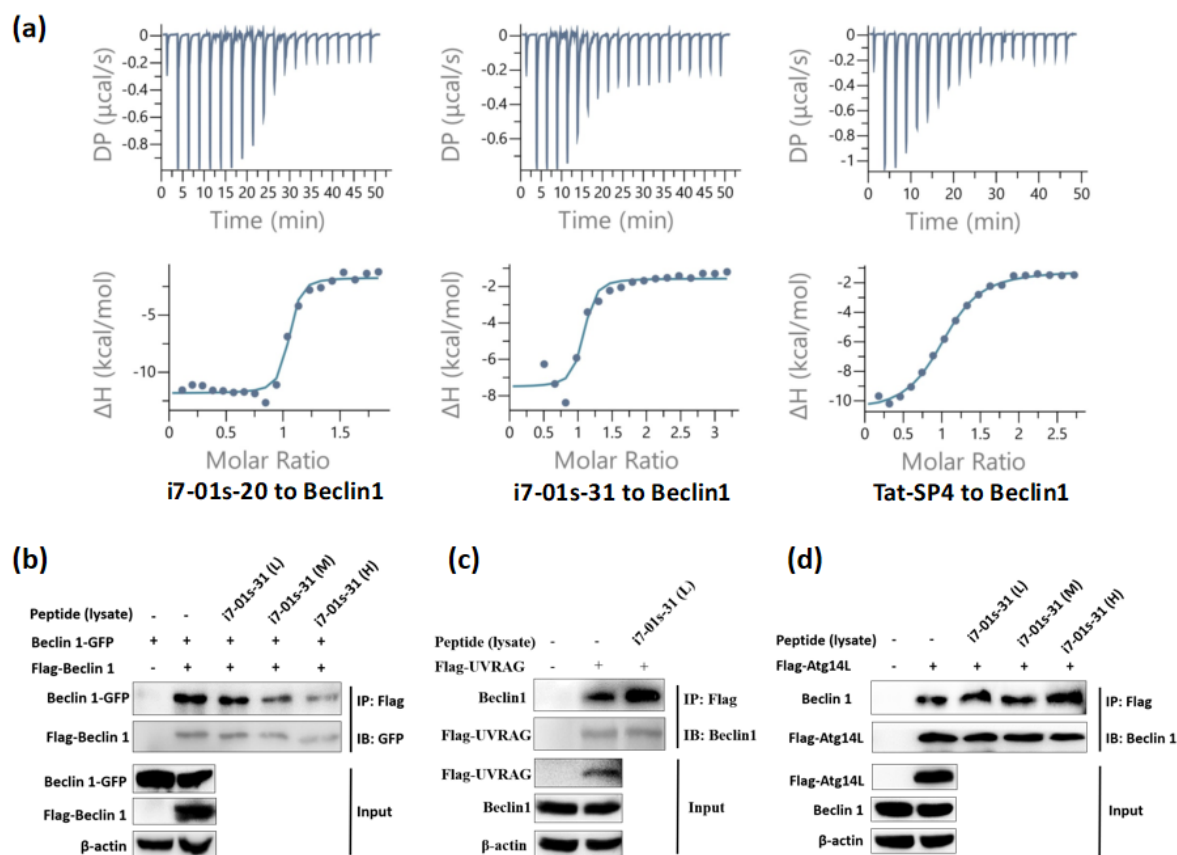
Figure 3. Stapled peptides with the i7-01s scaffold exhibited significantly enhanced binding affinity to Beclin 1 coiled-coil domain and promoted Beclin 1– Atg14L/UVRAG interaction. (a) Representative ITC profiles for i7-01s-20 and i7-01s-31 showed significantly enhanced binding affinity to Beclin 1 as compared to Tat-SP4. (b) Co-immunoprecipitation (co-IP) experiment indicated i7-01s-31 reduced Beclin 1 self-association. Flag- and GFP- tagged Beclin 1 were co-transfected into HEK293T cells, and their self-association was examined by co-IP. (c) & (d) Co-IP assays showed i7-01s-31 enhanced the Beclin 1- Atg14L/UVRAG interaction. Flag- UVRAG (c) or Flag- Atg14 (d) was transfected into HEK293T cell, and their interaction with endogenous Beclin 1 was assessed respectively by co-IP. Various concentrations of i7-01s-31 were added to the cell lysate before the IP procedure.
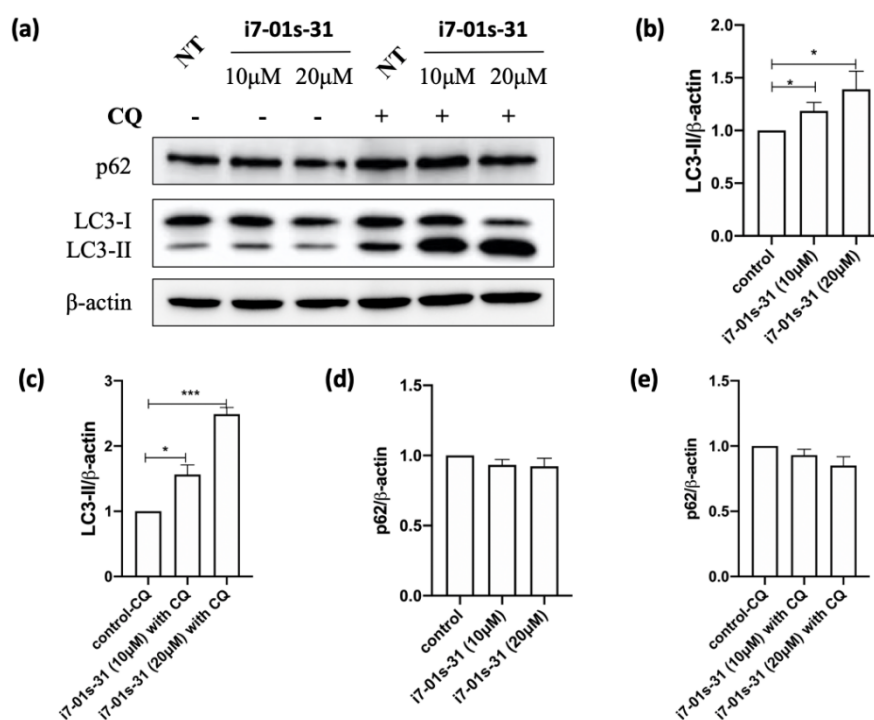
Figure 4. Peptides based on the i7-01s scaffold are effective inducers of autophagy. (a) Western blot to assess the p62 level and LC3 lipidation profile in HEK293T cells after treatment with 10- and 20- µM of i7-01s-31 for 3 hours, in the presence or absence of CQ. (b)&(c) Quantification of LC3 lipidation profiles from the Western blot data. (d)&(e) Quantification of p62 levels from the Western blot data. The levels of LC3-II or p62 were normalized to the β-actin level. Data are presented as mean ± SEM (n = 3).
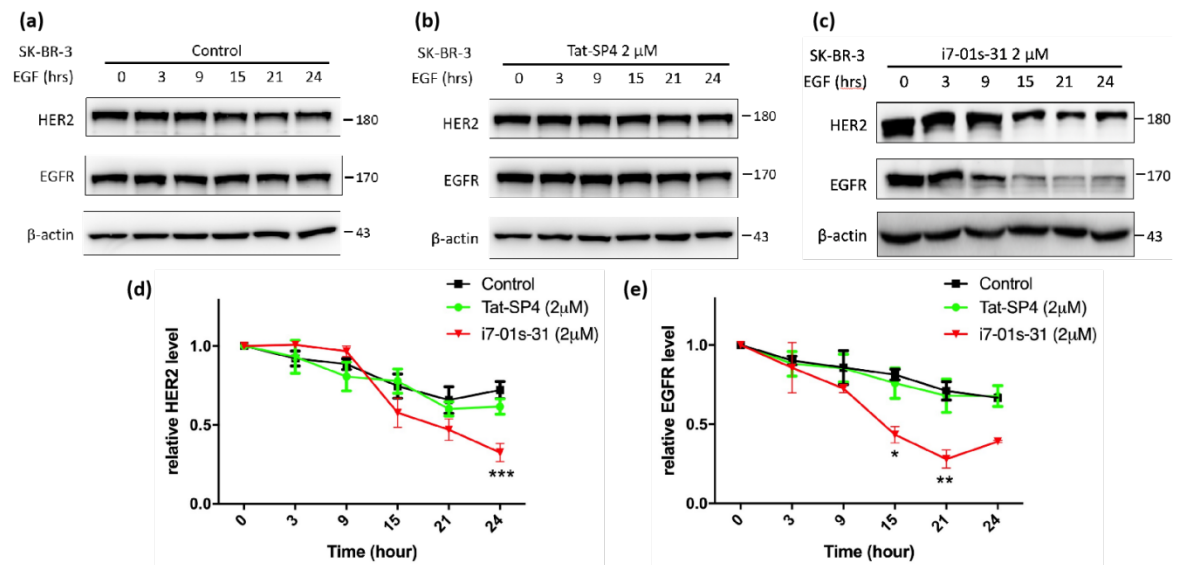
Figure 5. Peptides based on (i7-01s) scaffold are potent inducers of endolysosomal trafficking. (a-c) Western blot to assess the HER2 and EGFR levels in SKBR3 cells. Cells were starved overnight and were treated with 200 ng/mL EGF together with vehicle control (a), 2μM Tat-SP4 (b) , 2μM i7-01s-31 (c) or for the indicated times. (d & e) Time-dependent plots to quantify HER2 and EGFR degradation profiles after three independent experiments. The levels of HER2 (d) and EGFR (e) were normalized to the β-actin level at different time points and then further normalized to time 0, when the ligand EGF was added. Data are presented as mean ± SEM (n = 3).
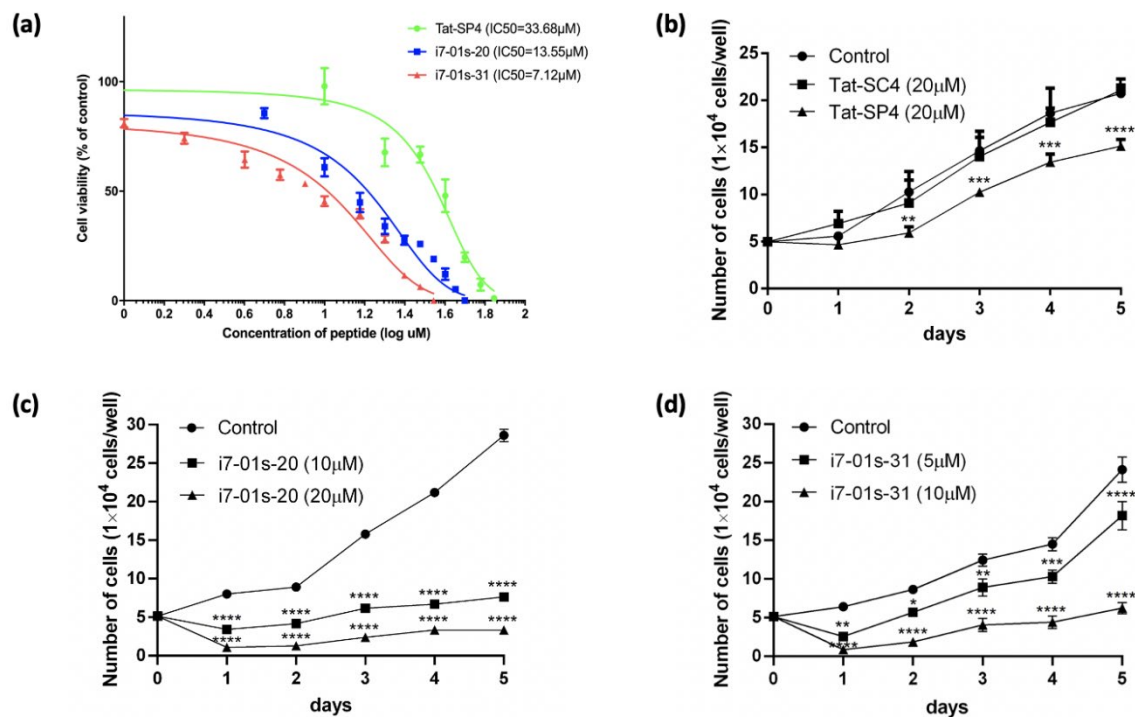
Figure 6. Peptides based on (i7-01s) scaffold exert potent anti-proliferative effect on HER2+ breast cancer cell line. (a) Trypan blue exclusion assay to assess the cytotoxicity IC50 of the indicated peptides in SKBR3 cells. Cells were treated with various concentrations of the indicated peptides for 24h. Cell numbers were manually counted by the trypan blue dye exclusion method using a hemocytometer. Data are presented as mean ± SD from three independent experiments. (b-d) Cell proliferation assay was performed over a time span of five days in SKBR3 cells after treatment with the indicated peptides. Cells were treated with the indicated peptides at day 0 and the cell number was calculated at the given time points. The assay was performed in 96 well plates with three independent measurements. Tat-SC4 is a control peptide with scrambled Tat-SP4 sequence but without the hydrocarbon staple.
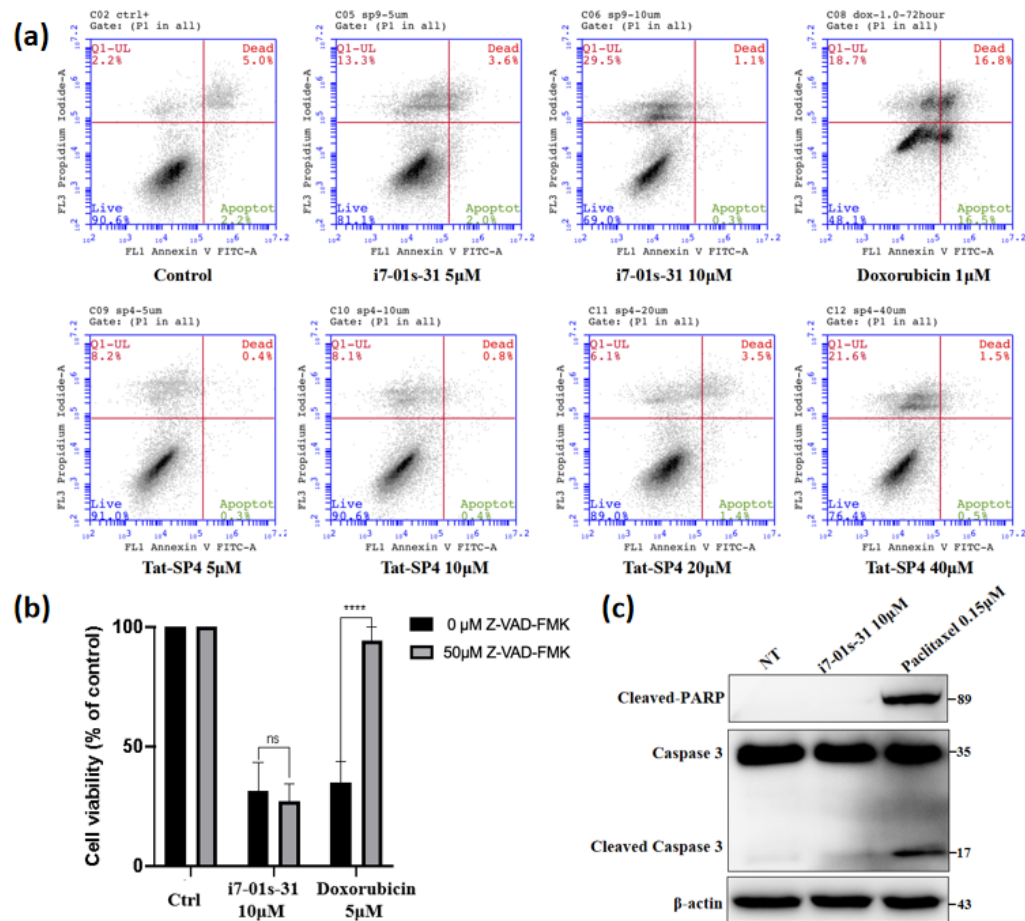
Figure 7. Peptides based on strategy (i7-01s) scaffold induce cell death with necrotic features. (a) Flow cytometry analysis with Annexin V FITC-PI staining was performed in SKBR3 cells after treatment of the indicated peptides for 24 hours. The percentage of dead cells (PI positive) in i7-01s-31 treatment groups were significantly increased compared with that of control, without notable changes in the population of apoptotic cells. (b) Trypan blue exclusion method to assess the viability of SKBR3 cells upon treatment with i7-01s-31 or doxorubicin for 24 hours, in the presence or absence of Z-VAD-FMK. Z-VAD-FMK: a pan-caspase inhibitor. (c)Western blot to assess the cleaved-PARP and caspase 3 levels in SKBR3 cells after treatment with 10μM of i7-01s-31 for 24 hours, or 0.15μM of paclitaxel for 48 hours. The expressions of cleaved-PARP and cleaved caspase-3 were induced by treatment of paclitaxel but not i7-01s-31.

Table 1. Sequence and binding affinity of newly designed stapled peptides with the i7-01s scaffold.

ID	SEQUENCE *	K_d (µM) #
Native-P1	RLIQELEDVEKNRKV	
Tat-SP4	Ac-[Tat]-RLISEL(R8)DREKQR(S5)A-NH₂	3.21 ± 0.49
i7-01s-02	Ac-[Tat]-RLIQ(R8)REDREK(S5)RAV-NH₂	0.86 ± 0.16
i7-01s-10	Ac-[Tat]-RLIQ(R8)REDREK(S5)RAR-NH₂	2.03 ± 0.56
i7-01s-12	Ac-[Tat]-RLIS(R8)REDREK(S5)RAE-NH₂	2.84 ± 0.48
i7-01s-20	Ac-[Tat]-RVIQ(R8)LVIIEK(S5)RDV-NH₂	**0.10 ±0.05**
i7-01s-30	Ac-[Tat]-RLLQ(R8)LKTVLK(S5)RSV-NH₂	No binding
i7-01s-31	Ac-[Tat]-VLFN(R8)LVDVIK(S5)RKV-NH₂	**0.33 ± 0.28**
i7-01s-34	Ac-[Tat]-RFIQ(R8)LEVVIK(S5)RSV-NH₂	No binding
i7-01s-36	Ac-[Tat]-RLIQ(R8)REDVEK(S5)RKR-NH₂	No binding
i7-01s-37	Ac-[Tat]-RLIQ(R8)KEDVEK(S5)RKR-NH₂	2.41 ± 0.35
i7-01s-45	Ac-[Tat]-RLKQ(R8)LEDVEK(S5)RKR-NH₂	1.41 ± 0.32
i7-01s-46	Ac-[Tat]-RLIQ(R8)KIDVEK(S5)RKR-NH₂	0.71 ± 0.23
i7-01s-54	Ac-[Tat]-ALIQ(R8)QEDVEK(S5)RKR-NH₂	311 ± 54.62
i7-01s-57	Ac-[Tat]-RRIQ(R8)MEDVLK(S5)RKR-NH₂	2.20 ± 0.36
i7-01s-58	Ac-[Tat]-RLIE(R8)REIVEK(S5)RKR-NH₂	0.61 ± 0.17
i7-01s-64	Ac-[Tat]-RLII(R8)QEDVEK(S5)RKR-NH₂	356 ± 78.53
i7-01s-70	Ac-[Tat]-RLIQ(R8)KGDVEL(S5)RKR-NH₂	2.14 ± 0.47
i7-01s-75	Ac-[Tat]-RLIY(R8)MEDVEK(S5)RKR-NH₂	1.29 ± 0.40

* Each peptide was synthesized with Tat sequence (YGRKKRRQRRR) added at the N-terminal. The colored residues indicate mutations as compared to Native-P1.

The binding affinity (K_d) of each designed stapled peptide was measured by ITC assay and compared to Native-P1 and Tat-SP4. The two strongest K_d values, i.e. for i7-01-20 and i7-01s-34, are highlighted in bold.

ASSOCIATED CONTENT

Supplemental Figures S1-S6.

Supplemental Table ST1.

AUTHOR INFORMATION

Corresponding Author

*Correspondence should be addressed to Y.Z. (yanxiang.zhao@polyu.edu.hk) and R.W. (wangrx@fudan.edu.cn).

Author Contributions

QY, GF and YL carried out the molecular design and modeling work and also provided the samples of the designed stapled peptides. XQ, XZ, YY, NL and WX conducted biochemical and cellular assays. QY and XQ wrote sections of the manuscript. YZ and RW supervised the project, designed the experiments, analyzed the data, and completed the manuscript. All authors have given approval to the final version of the manuscript. [†]These authors contributed equally to this work.

Notes

The authors have filed patent applications in U.S. and China based on this work.

ACKNOWLEDGEMENT

References

1. Levine B, Liu R, Dong X, & Zhong Q (2015) Beclin orthologs: integrative hubs of cell signaling, membrane trafficking, and physiology. *Trends Cell Biol* 25(9):533-544.
2. Liang XH*, et al.* (1998) Protection against fatal Sindbis virus encephalitis by beclin, a novel Bcl-2-interacting protein. *J Virol* 72(11):8586-8596.
3. He C & Levine B (2010) The Beclin 1 interactome. *Curr Opin Cell Biol* 22(2):140-149.
4. Funderburk SF, Wang QJ, & Yue Z (2010) The Beclin 1-VPS34 complex--at the crossroads of autophagy and beyond. *Trends Cell Biol* 20(6):355-362.
5. Levine B & Kroemer G (2019) Biological Functions of Autophagy Genes: A Disease Perspective. *Cell* 176(1-2):11-42.
6. Dikic I & Elazar Z (2018) Mechanism and medical implications of mammalian autophagy. *Nat Rev Mol Cell Biol* 19(6):349-364.
7. Mizushima N & Levine B (2020) Autophagy in Human Diseases. *N Engl J Med* 383(16):1564-1576.
8. Liang XH*, et al.* (1999) Induction of autophagy and inhibition of tumorigenesis by beclin 1. *Nature* 402(6762):672-676.
9. Yue Z, Jin S, Yang C, Levine AJ, & Heintz N (2003) Beclin 1, an autophagy gene essential for early embryonic development, is a haploinsufficient tumor suppressor. *Proc Natl Acad Sci U S A* 100(25):15077-15082.
10. Wei Y*, et al.* (2013) EGFR-mediated Beclin 1 phosphorylation in autophagy suppression, tumor progression, and tumor chemoresistance. *Cell* 154(6):1269-1284.
11. Vega-Rubin-de-Celis S*, et al.* (2018) Increased autophagy blocks HER2-mediated breast tumorigenesis. *Proc Natl Acad Sci U S A* 115(16):4176-4181.
12. Liang C*, et al.* (2006) Autophagic and tumour suppressor activity of a novel Beclin1-binding protein UVRAG. *Nat Cell Biol* 8(7):688-699.
13. Zhong Y*, et al.* (2009) Distinct regulation of autophagic activity by Atg14L and Rubicon associated with Beclin 1-phosphatidylinositol-3-kinase complex. *Nat Cell Biol* 11(4):468-476.

14. Matsunaga K, *et al.* (2009) Two Beclin 1-binding proteins, Atg14L and Rubicon, reciprocally regulate autophagy at different stages. *Nat Cell Biol* 11(4):385-396.
15. Li X, *et al.* (2012) Imperfect interface of Beclin1 coiled-coil domain regulates homodimer and heterodimer formation with Atg14L and UVRAG. *Nat Commun* 3:662.
16. Wu S, *et al.* (2018) Targeting the potent Beclin 1-UVRAG coiled-coil interaction with designed peptides enhances autophagy and endolysosomal trafficking. *Proc Natl Acad Sci U S A* 115(25):E5669-E5678.
17. Walensky LD & Bird GH (2014) Hydrocarbon-stapled peptides: principles, practice, and progress. *J Med Chem* 57(15):6275-6288.
18. Walensky LD, *et al.* (2004) Activation of apoptosis in vivo by a hydrocarbon-stapled BH3 helix. *Science* 305(5689):1466-1470.
19. Walensky LD, *et al.* (2006) A stapled BID BH3 helix directly binds and activates BAX. *Mol Cell* 24(2):199-210.
20. LaBelle JL, *et al.* (2012) A stapled BIM peptide overcomes apoptotic resistance in hematologic cancers. *J Clin Invest* 122(6):2018-2031.
21. Cohen NA, *et al.* (2012) A competitive stapled peptide screen identifies a selective small molecule that overcomes MCL-1-dependent leukemia cell survival. *Chem Biol* 19(9):1175-1186.
22. Lee S, Braun CR, Bird GH, & Walensky LD (2014) Photoreactive stapled peptides to identify and characterize BCL-2 family interaction sites by mass spectrometry. *Methods Enzymol* 544:25-48.
23. Stewart ML, Fire E, Keating AE, & Walensky LD (2010) The MCL-1 BH3 helix is an exclusive MCL-1 inhibitor and apoptosis sensitizer. *Nat Chem Biol* 6(8):595-601.
24. Moellering RE, *et al.* (2009) Direct inhibition of the NOTCH transcription factor complex. *Nature* 462(7270):182-188.
25. Bernal F, Tyler AF, Korsmeyer SJ, Walensky LD, & Verdine GL (2007) Reactivation of the p53 tumor suppressor pathway by a stapled p53 peptide. *J Am Chem Soc* 129(9):2456-2457.
26. Takada K, *et al.* (2012) Targeted disruption of the BCL9/beta-catenin complex inhibits oncogenic Wnt signaling. *Sci Transl Med* 4(148):148ra117.
27. Baek S, *et al.* (2012) Structure of the stapled p53 peptide bound to Mdm2. *J Am Chem Soc* 134(1):103-106.
28. Chang YS, *et al.* (2013) Stapled alpha-helical peptide drug development: a potent dual inhibitor of MDM2 and MDMX for p53-dependent cancer therapy. *Proc Natl Acad Sci U S A* 110(36):E3445-3454.
29. Nomura W, *et al.* (2013) Cell-permeable stapled peptides based on HIV-1 integrase inhibitors derived from HIV-1 gene products. *ACS Chem Biol* 8(10):2235-2244.
30. Long YQ, *et al.* (2013) Design of cell-permeable stapled peptides as HIV-1 integrase inhibitors. *J Med Chem* 56(13):5601-5612.
31. Zhang H, *et al.* (2011) Antiviral activity of alpha-helical stapled peptides designed from the HIV-1 capsid dimerization domain. *Retrovirology* 8:28.
32. Bhattacharya S, Zhang H, Debnath AK, & Cowburn D (2008) Solution structure of a hydrocarbon stapled peptide inhibitor in complex with monomeric C-terminal domain of HIV-1 capsid. *J Biol Chem* 283(24):16274-16278.
33. Phillips C, *et al.* (2011) Design and structure of stapled peptides binding to estrogen receptors. *J Am Chem Soc* 133(25):9696-9699.
34. Danial NN, *et al.* (2008) Dual role of proapoptotic BAD in insulin secretion and beta cell survival. *Nat Med* 14(2):144-153.

35. Bird GH*, et al.* (2020) Hydrocarbon-Stitched Peptide Agonists of Glucagon-Like Peptide-1 Receptor. *ACS Chem Biol* 15(6):1340-1348.
36. Amaravadi R, Kimmelman AC, & White E (2016) Recent insights into the function of autophagy in cancer. *Genes Dev* 30(17):1913-1930.
37. Poillet-Perez L & White E (2019) Role of tumor and host autophagy in cancer metabolism. *Genes Dev* 33(11-12):610-619.
38. Kimmelman AC & White E (2017) Autophagy and Tumor Metabolism. *Cell Metab* 25(5):1037-1043.
39. Galluzzi L*, et al.* (2015) Autophagy in malignant transformation and cancer progression. *EMBO J* 34(7):856-880.
40. Goldsmith J, Levine B, & Debnath J (2014) Autophagy and cancer metabolism. *Methods Enzymol* 542:25-57.
41. Rojas-Puentes LL*, et al.* (2013) Phase II randomized, double-blind, placebo-controlled study of whole-brain irradiation with concomitant chloroquine for brain metastases. *Radiat Oncol* 8:209.
42. Boone BA*, et al.* (2015) Safety and Biologic Response of Pre-operative Autophagy Inhibition in Combination with Gemcitabine in Patients with Pancreatic Adenocarcinoma. *Ann Surg Oncol* 22(13):4402-4410.
43. Wolpin BM*, et al.* (2014) Phase II and pharmacodynamic study of autophagy inhibition using hydroxychloroquine in patients with metastatic pancreatic adenocarcinoma. *Oncologist* 19(6):637-638.